ECG Source Location Clustering Based on Position Vectors and Forward Transfer Matrices

Takano N, H-G Puurtinen, M Rautiainen,
J Hyttinen, J Malmivuo

Ragnar Granit Institute, Tampere University of Technology,
Tampere, Finland

Abstract

Heart model segmentation methods concerning ECG source-to-measurement forward transfer modeling are discussed. The k-means clustering technique was adopted to classify all discrete points forming a heart model with respect to their position vectors or source-to-measurement transfer matrices. The clusters were formed in heart models of end-systolic and end-diastolic cardiac phases. The minimum number of clusters for different lead systems, cardiac phases and in volume conductor models determined for least square error approximation of non-clustered (original) transfer model are tabulated. These numbers suggested that the number current dipole sources could be reduced to less than 10% of that of the source locations. Some of the heart models segmented by the resulting clusters are presented at the end of this article.

1. Introduction

Since sensitivities of ECG leads are dependent on ECG source locations, ECG source-to-measurement transfer matrices in forward transfer models also vary by the source locations. In order to analyze such sensitivity distributions and/or to reduce the number of sources in forward transfer model, the present study applies the *k*-means clustering technique to the transfer matrices or position vectors of the source locations, and approximates the transfer matrices in each cluster by one matrix. There are already definitions of segmentations of the left ventricle [1], but they are based on anatomical features for myocardial infarction studies, not specially for forward problem of ECG. The approach introduced here is mathematical one, and can be applied to the entire heart.

2. Theory and method

2.1. Source-to-measurement transfer models

In ECG source-to-measurement forward transfer models, the measurements are computed by liner transformation of ECG sources. Each solution can be given as a vector comprising ECG voltages in an ECG lead system of multiple leads. Current dipole sources are considered in the present study.

2.1.1 Non-clustered model

In a non-clustered model, the sources at locations in a heart model are transformed into measurements:

$$\mathbf{v} = \sum_{l=1}^{L} \mathbf{C}_l \mathbf{u}_l, \tag{1}$$

$\mathbf{v}$: forward solution in non-clustered model;
l : index of source location;
L : the number of source locations;
$\mathbf{C}_l$: source-to-measurement transfer matrix at location l;
$\mathbf{u}$: current dipole source vector.

2.1.2 Clustered model

In a clustered model, ECG source locations are classified into subsets, and sources at locations in each subset can be summed up before the transformations:

$$\hat{\mathbf{v}} = \sum_{k=1}^{K} \hat{\mathbf{C}}_k \sum_{l \in \mathcal{K}_k} \mathbf{u}_l, \tag{2}$$

$\hat{\mathbf{v}}$: forward solution in clustered model using $\hat{\mathbf{C}}_{k=1:K}$;
k : index of mutually associated subset and cluster;
K : the number of subsets or of clusters;
$\hat{\mathbf{C}}_k$: transfer matrix optimized for cluster k;
$\mathcal{K}$: subset of source locations.

The sources to be considered in a clustered model is reduced in such a sense that $K < L$.

0276–6547/02 $17.00 © 2002 IEEE

Computers in Cardiology 2002;29:313–316.

2.2. LS approximation of transfer matrices

$\hat{\mathbf{C}}_{k=1:K}$ of clusters are optimized for the least squared (LS) error approximations of $\mathbf{C}_{l\in\mathcal{K}_k}$ for each k. They are obtained by numerical averaging of $\mathbf{C}_l$ in each $\mathcal{K}_k$:

$$\hat{\mathbf{C}}_k = \frac{1}{L_k}\sum_{l\in\mathcal{K}_k}\mathbf{C}_l,\ k=1:K, \tag{3}$$

where L_k is the number of location indices in $\mathcal{K}_k$.

As an evaluation of the approximations, approximation error ratio, ξ_K, is defined here. It is essentially the summation of squared Euclidean norms of the approximation errors, $\mathbf{C}_l - \hat{\mathbf{C}}_k$:

$$\xi_K = \frac{\sum_{k=1}^{K}\sum_{l\in\mathcal{K}_k}\|\mathbf{C}_l - \hat{\mathbf{C}}_k\|_E^2}{\sum_{l=1}^{L}\|\mathbf{C}_l\|_E^2} \tag{4}$$

The denominator is for such a normalization that $0 \le \xi_K \le 1$. The suffix of ξ_K indicates the number of clusters used for the approximations.

2.3. *k*-means clustering

In order to form subsets $\mathcal{K}_{k=1:K}$, the *k*-means clustering technique [2] was employed. It classifies indices $l = 1:L$ of data samples, denoted here by $\mathbf{x}_l$, of interest to form clusters. Successfully formed clusters exhibit high homogeneity of $\mathbf{x}_l$ within cluster and high heterogeneity between clusters. This method iterates the steps listed here:

1. Centroid, $\dot{\mathbf{x}}_k$, is calculated in each cluster:

$$\dot{\mathbf{x}}_k = \frac{1}{L_k}\sum_{l\in\mathcal{K}_k}\mathbf{x}_l,\ k=1:K, \tag{5}$$

2. $l = 1:L$ are classified by "closeness" to the centroids:

$$\mathcal{K}_k = \{l | k = \arg\min_{k'}\|\mathbf{x}_l - \dot{\mathbf{x}}_{k'}\|_E\},\ k=1:K, \tag{6}$$

3. If $\dot{\mathbf{x}}_{k=1:K}$ have converged, quit, otherwise return to 1.

Two types of clusters were formed by characteristics of source locations as listed below.

Transfer matrix-based clustering : $\mathbf{C}_{l=1:L}$ in non-clustered model were used as the characteristic $\mathbf{x}$ seen in (5) and (6); in this clustering (5) is identical to (3);

Position vector-based clustering : Position vectors in a Cartesian coordinate system of locations, $l = 1:L$, were clustered, $\hat{\mathbf{C}}_{k=1:K}$ of these clusters being determined and evaluated by (3) and (4).

2.4. Experiment procedure

Each clustering process commenced with $K = 1$. After the clusters converged, K was incremented by 1 and the clustering was executed again. Transfer matrix-based clustering process stopped when $\xi_K \le 0.01$ was obtained, and position vector-based stopped when $\xi_K \le 0.1$.

3. Study material

3.1. Thorax-heart models

The transfer matrices were computed in the volume conductor thorax models listed here:

i-sys : inhomogeneous, end-systolic;
i-dia : inhomogeneous, end-diastolic;
h-sys : homogeneous, end-systolic;
h-dia : homogeneous, end-diastolic.

Two of them are inhomogeneous conductor models constructed from magnetic resonance images for the finite difference method (FDM) computing, and the other assumed an infinite extent of homogeneous conductivity. The origin of the four is i-sys model, which contains a heart model of end-systolic cardiac phase. Except for the heart model of end-diastolic phase, i-dia model is identical with i-sys. All FDM grid nodes forming a heart model were used as source locations. The end-systolic heart model was formed by 12032 location points and the end-diastolic heart model by 13120. In the homogeneous models electrodes and source locations were set the same as the inhomogeneous models.

3.2. Lead systems

Since the transfer matrix is formed for a specific lead system, clustering analysis was performed for several lead systems, including these in the list:

bsm120 : A body surface mapping (BSM) lead system [3] comprising 120 unipolar leads;
krn5 : 5 leads selected by Kornreich's group for multiple diagnosis [4], a subset of bsm120;
limb3 : 3 unipolar limb leads;
prec6 : 6 precordial leads in the standard leads;
limb3 + prec6 : combination of limb3 and prec6;
std12 : standard 12 ECG leads, including prec6, and augmented limb and bipolar limb leads;
frank7 : unipolar leads at 7 electrode sites defined for Frank vector leads, using the Wilson central terminal;
frank : Frank vector leads.

4. Results

As K was incremented, ξ_K decreased monotonously. The minimum K to obtain certain values of ξ_K are summarized in Table 1, which may suggest the number of clusters (or sources) necessary for constructing forward transfer models as reduced versions of the original (non-clustered) model. Position vector-based clusters for $\xi_K \le 0.1$ were so many as the transfer matrix-based clusters for far lower ξ. $\min K$ did not always reflect the number of leads or electrode sites in the lead systems.

Cluster partitions in a heart model differed by clustering methods and conductivity models even if ξ_K or K are the same, for instance $\xi_K \leq 0.1$ and $K \approx 750$ seen in Figure 1. The position vector-based clusters were almost equally sized in each clustered model while the transfer matrix-based clusters were smaller in regions closer to electrodes. In the inhomogeneous models with transfer matrix-based clustering, locations near to and far from a boundary of the heart were often classified into different clusters; such partitions were not seen in the homogeneous models. Bear in mind, identical sources at different locations in each cluster produce approximately the same measurements.

5. Conclusion

Although the position vector-based clustering, as it is defined, made spatially clear partitions in the heart models, it was not so efficient for ECG source reduction as the transfer matrix-based clustering. The transfer matrix-based clusters had their sizes varied by regions in the heart and formed intricate spatial partitions, which were also affected by inhomogeneous conductivities in the thorax-heart model. It was also observed that increase or decease of the number of clusters sufficient for forward transfer model could not be expected directly from change in the number of leads or electrodes in the lead system.

References

[1] Startt/Selvester RH, Wagner GS, Ideker RE. Myocardial infarction. In Macfarlane PW, Lawrie TDV (eds.), Comprehensive Electrocardiography: Theory and Practice in Health and Disease, volume 1, first edition. Elmsford, New York, U.S.A.: Pergamon Press, 1989; 565–629.

[2] Rabiner LR, Juang BH. Fundamentals of Speech Recognition. Englewood Cliffs, New Jersey, U.S.A.: Prentice-Hall, 1993; 122–132.

[3] Montague TJ, Smith ER, Cameron DA, Rautaharju PM, Klassen GA, Felmington CS, Horaceck BM. Isointegral analysis of body surface maps: Surface distribution and temporal variability in normal subjects. Circulation May 1981;63(5):1166–1172.

[4] Korneich F, Montague TJ, Pentti Rautaharju MK, Horaceck MB, Taccardi B. Multigroup diagnosis of body surface potential maps. Journal of Electrocardiology 1989;22 Supplement:169–178.

Address for correspondence:

TAKANO Noriyuki
Ragnar Granit Institute, Tampere University of Technology
P.O. Box 692 FIN-33101 Tampere Finland
tel: +358-3-3115 2524
fax: +358-3-3115 2162
noriyuki.takano@tut.fi

i-sys model, $L = 12032$ source locations						
		PVB	TMB			
Lead Config	N_L/N_E	0.1	0.1	0.05	0.03	0.01
bsm120	120/120	718	77	291	781	1899
krn5	5/8	846	24	94	222	997
limb3	3/3	41	4	19	64	572
prec6	6/9	1008	32	109	260	990
limb3 + prec6	9/9	958	33	128	274	1077
std12	12/9	884	33	138	312	1268
frank7	7/9	1054	25	94	237	1055
frank	3/7	498	15	65	195	1192
i-dia model, $L = 13120$ source locations						
Lead Config	N_L/N_E	0.1	0.1	0.05	0.03	0.01
bsm120	120/120	1318	100	349	700	2033
krn5	5/8	2365	27	94	225	959
limb3	3/3	113	7	23	70	666
prec6	6/9	1877	30	127	286	965
limb3 + prec6	9/9	1730	33	120	297	1019
std12	12/9	1551	35	154	327	1196
frank7	7/9	1743	26	91	202	933
frank	3/7	994	16	63	194	1229
h-sys model, $L = 12032$ source locations						
Lead Config	N_L/N_E	0.1	0.1	0.05	0.03	0.01
bsm120	120/120	37	24	66	147	764
krn5	5/8	39	19	53	115	601
limb3	3/3	1		2	4	15
prec6	6/9	55	20	58	133	674
limb3 + prec6	9/9	54	20	57	136	669
std12	12/9	48	19	55	127	662
frank7	7/9	54	21	58	128	669
frank	3/7	11	4	14	32	198
h-dia model, $L = 13120$ source locations						
Lead Config	N_L/N_E	0.1	0.1	0.05	0.03	0.01
bsm120	120/120	53	29	82	187	948
krn5	5/8	52	21	56	128	627
limb3	3/3	1			4	17
prec6	6/9	72	26	70	164	782
limb3 + prec6	9/9	69	26	69	169	767
std12	12/9	68	25	69	156	742
frank7	7/9	86	27	75	168	683
frank	3/7	31	8	23	60	280

Table 1. The minimum number of clusters, K, to obtain approximation error ratio ξ_K of transfer matrices ≤ 0.1 by the position vector-based (PVB) clustering and 0.1 to 0.01 by the transfer matrix-based (TMB) clustering in i-sys, i-dia, h-sys, h-dia thorax-heart models each containing a heart model formed by L source locations. These minimum numbers were evaluated for the lead systems whose number of leads and electrode sites are indicated by N_L and N_E, respectively, in the second column.

Inhomogeneous thorax model with end-systolic heart model

position vector-based clusters for $\xi_K \leq 0.1$, $K = 718$

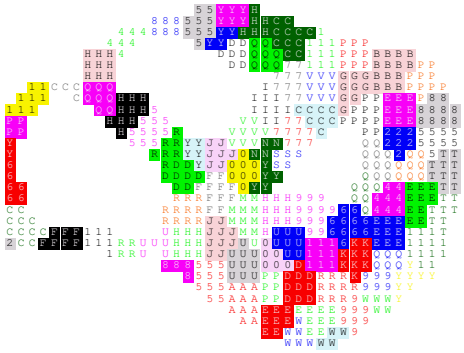

transfer matrix-based clusters for $\xi_K \leq 0.1$, $K = 77$

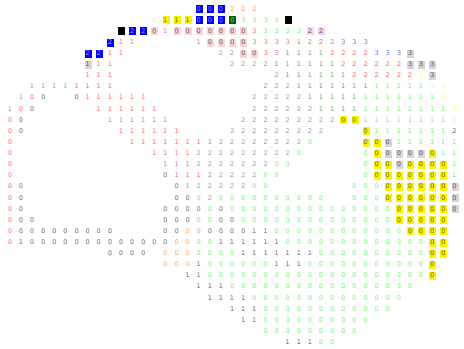

transfer matrix-based clusters for $\xi_K \leq 0.03$, $K = 781$

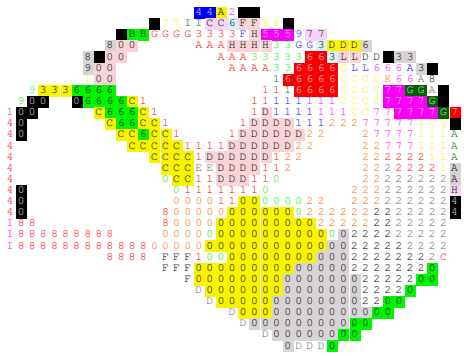

Homogeneous thorax model with end-systolic heart model

position vector-based clusters for $\xi_K \leq 0.1$, $K = 37$

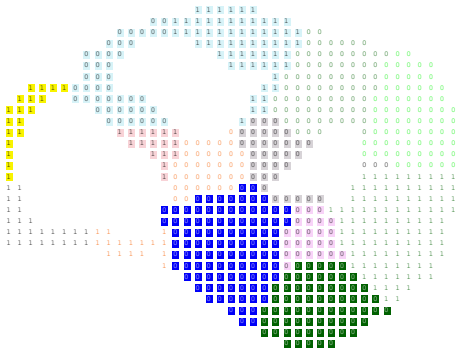

transfer matrix-based clusters for $\xi_K \leq 0.1$, $K = 24$

transfer matrix-based clusters for $\xi_K \leq 0.01$, $K = 764$

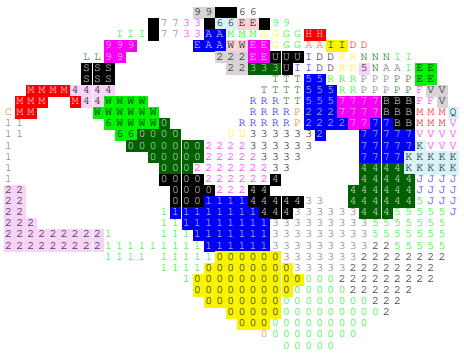

Figure 1. Transverse views of clustered heart models (anterior side is up, and left side of the body is right-hand side of the slice). On the left-hand side are results in i-sys model, on the right-hand side are those in h-sys. These indicate classifications of locations according to the minimum K of clusters to obtain ξ_K less than or equal to a given value written on each slice picture regarding approximation of $\mathbf{C}$ in non-clustered model for bsm120 lead system (see also Table 1). Combinations of character, fore- and background colors indicate clusters into which the locations are classified. These combinations are consistent in each clustering result only. They do not indicate any characteristic of the clusters, except for that the squares filled in black in the anterior regions indicate clusters each consisting of only one location.